

## Spherical-harmonics mode decomposition of neural field equations

Daniele Daini,<sup>1</sup> Giacomo Ceccarelli,<sup>2</sup> Enrico Cataldo<sup>1,2,\*</sup> and Viktor Jirsa<sup>1</sup>

<sup>1</sup>UMR Inserm 1106, Aix-Marseille Université, Faculté de Médecine, 27, Boulevard Jean Moulin, 13005 Marseille, France

<sup>2</sup>Physics Department, Largo B. Pontecorvo 3, University of Pisa, 56127 Pisa, Italy



(Received 4 July 2019; published 6 January 2020)

Large-scale neural networks can be described in the spatial continuous limit by neural field equations. For large-scale brain networks, the connectivity is typically translationally variant and imposes a large computational burden upon simulations. To reduce this burden, we take a semiquantitative approach and study the dynamics of neural fields described by a delayed integrodifferential equation. We decompose the connectivity into spatially variant and invariant contributions, which typically comprise the short- and long-range fiber systems, respectively. The neural fields are mapped on the two-dimensional spherical surface, which is choice consistent with routine mappings of cortical surfaces. Then, we perform mathematically a mode decomposition of the neural field equation into spherical harmonic basis functions. A spatial truncation of the leading orders at low wave number is consistent with the spatially coherent pattern formation of large-scale patterns observed in simulations and empirical brain imaging data and leads to a low-dimensional representation of the dynamics of the neural fields, bearing promise for an acceleration of the numerical simulations by orders of magnitude.

DOI: [10.1103/PhysRevE.101.012202](https://doi.org/10.1103/PhysRevE.101.012202)

### I. INTRODUCTION

Neuronal dynamics encompass many temporal and spatial scales and at each scale several theoretical and computational models, with a variable level of details, have been developed [1–4]. When modeling large-scale neural networks, such as cortical, thalamocortical, or cerebellar networks, some approaches describe the single neuron of the network with a conductance-based model or with a simplified version of it, but in both cases the system becomes rapidly very complex [5–7]. The number of neurons even in small systems like the aforementioned ones is prohibitively high. Thereby, to cope with systems of such complexity, an alternative description is worthwhile and possible, under certain constraints. In these cases, the macroscopic state variables are the mean firing rates or population activities and these descriptions are known as *neural mass models* [8–15].

In order to describe the neural activity underpinning complex behavior or cognitive functions [16], a further step consists in the implementation of interacting neural mass models, in which the neural signals between the different populations depend on the brain connectivity [17–21] and are characterized by time delays, ranging from fractions to tenths of milliseconds [22–26] and due mainly to the finite value of action potential transmission speeds [27,28]. Due to the high spatial density of the number of neurons in the cerebral cortex, it is possible to represent the mean neural activity as a continuous function of space, which must satisfy specific integrodifferential equations [29–31]. In practice, *neural field models* are needed when considering a dense ensemble of neural masses. The relevance of these models resides in their link with important neural recording techniques, such as elec-

troencephalogram (EEG) and functional magnetic resonance imaging (fMRI) [32,33]. Moreover, a great number of neural processes underlying, for example, working memory and perception can be adequately described by means of neural field equations [34,35].

In recent years a lot of new experimental data on the intricate network structure of cerebral matter have become available, allowing a realistic description of neural connections as weighted matrices of links among different cortical areas [17,20]. The so-called connectome is the finite set of all structural connections including their connection weights. In conjunction with the link's track lengths, which allow the inference of signal transmission delays, the connectome spans a space-time structure critical for the synchronization dynamics of the network. The introduction of these data into the models has led to new and more specific field equations. The distinctive features of currently used models in neural dynamics are the presence of continuously distributed delays and the split of the integral kernel, which represents, in some cases, the physiological connectivity with two distinct features.

Along this line of research, in a previous work [36] a study of a neural field equation was pursued in which the connectivity was divided in two components: A local one, defined by its short-range nature, and a global one, corresponding to long-range links [37,38]. Finally this model considered the spatially dependent delay effect, due to the transmission of signals along neuronal fibers, as simply given by the distance between two points of the local field divided by the propagation speed. The work focused on the perturbation to a resting state condition, thus enabling the mathematical tools of linear analysis. In particular it has investigated the contribution to the power spectrum of the field potential, showing that local connectivity underlies the power-law behavior (with an exponent of  $-2$ ) while the global connectivity is at the origin of the frequency

\*enrico.cataldo@unipi.it

peaks. Some authors have also studied the behavior of the power spectrum when the thalamocortical connectivity is also taken into account [39].

In the present paper we extend the mathematical analysis developed in Ref. [36] from the one-dimensional linear spatial domain to the two-dimensional spherical surface. This is relevant for two reasons: First, a closer connection with experimental data is accomplished, because the existence of inflation algorithms makes it possible to map the intricate convolution structure of the cortex onto a sphere [40,41]. Second, Jirsa's analysis demonstrated that the effects of the space-time structure of the connectome can be absorbed to a large degree in the coefficients of an appropriately chosen spatial mode decomposition. This process, in conjunction with a truncation of the mode decomposition, promises an enormous numerical information compression and reduction of the complexity of the system. There is a conspicuous number of papers treating low-order truncation of modal dynamics and mode coupling by inhomogeneity (see, for example, Refs. [26,39,42]).

Here we derive the mathematical form of such a compressed representation. To do so, we perform a mode decomposition on the basis of spherical harmonics for the neural field. Spherical harmonics have already been used in the literature of neural fields because of their natural relationship with the topology of the brain [43,44]. A detailed stability analysis of the model on a spherical domain was given in Ref. [45], where the connectivity kernel was taken as rotationally invariant, at variance with the present work.

Apart from the obvious topological reason, there are other motivations for using spherical harmonics:

(1) Since the local connectivity, when properly approximated, gives rise to a diffusive dynamics, we use a basis of eigenfunctions for the Laplacian operator. Such a decomposition leads to a form of the field equations which can be the starting point for a truncation approximation; in particular, being interested in local electrical brain activities, possibly for a comparison with experimental data, we can disregard all the fine structure which is encoded in the spherical harmonics with a high resolution, that is, those of higher order.

(2) The time evolution of the mode coefficients shows a dissipative behavior, which grows as the squared order of the mode. We exploit this fact in dissipative systems to reduce the memory involved in numerical simulations via the truncation technique.

(3) The use of spherical harmonics in neural field models is not suggested only by mathematical convenience; there is also experimental insight supporting their natural emergence: In recent work [46], spherical harmonics were able to describe the principal components in the analysis of stationary electrical activity during non-REM sleep.

The paper is organized as follows. In Sec. II we specify our model, giving an insight of its physiological foundations. In Sec. III we study, as a toy model, the case of a circular domain. The reason is that this domain is compact like the spherical one, which is our final interest, so that it shows the logic of our analyses, but, being one dimensional, all the technical details are greatly reduced. The results of this section are the approximation of the local connectivity term and the mode decomposition of the global field equation. In Sec. IV we apply exactly the same analyses done for the circumference to

the spherical domain obtaining the analogous results. Finally, in Sec. VI we draw our conclusions, commenting on the usefulness of our analyses in connection with current brain models. Our mathematical results are almost exact and can be used as the starting point for different types of approximations and numerical computations.

## II. NEURAL FIELD EQUATION

In this paper we study the neural field equation [36]

$$\begin{aligned} \dot{\psi}(x, t) + \epsilon\psi(x, t) &= \int_{\mathcal{D}} W_{\text{hom}}(|x - y|) S[\psi(y, t - |x - y|/c)] dy \\ &+ \int_{\mathcal{D}} W_{\text{het}}(x, y) S[\psi(y, t - |x - y|/v)] dy, \end{aligned} \quad (1)$$

where the dot denotes the time derivative. Here  $\mathcal{D}$  represents a general physical domain and  $x, y$  are spatial variables relative to that domain. The function  $\psi(x, t)$  measures the local field potential of neural activity at time  $t$  and position  $x$  and it is a coarse-grained mean of the firing rates of a population of neurons. The constant  $\epsilon$  represents the temporal rate of decay of the local field potential  $\psi(x, t)$ . The integral kernels  $W_{\text{hom}}$  and  $W_{\text{het}}$  are called the *homogeneous* and *heterogeneous* brain connectivities, respectively, and are assumed to be known functions, while the parameters  $c$  and  $v$  denote the transmission speeds through the two fiber systems. Finally,  $S[\psi]$  is the activity function, which is generally approximated with a sigmoid.

We now give some examples of brain connectivities. Since  $W_{\text{hom}}$  represents the short-range cortical connectivity, its form can thus be assumed to be translation invariant and fast decaying [18]. A common choice for  $W_{\text{hom}}$  is

$$W_{\text{hom}}(z) = N(\sigma)e^{-|z|/\sigma}, \quad (2)$$

where  $\sigma$  is the typical length scale and  $N(\sigma)$  is a domain-dependent normalization factor, so that  $\int_{\mathcal{D}} W_{\text{hom}}(z) dz = 1$ . Instead, since  $W_{\text{het}}$  represents the long-range cortical connectivity, no general assumption is justified on a physiological basis [18]. For  $W_{\text{het}}$  the following pairwise point form is often assumed:

$$W_{\text{het}} = \sum_{ij}^{\mathcal{L}} \mu_{ij} \delta(x - x_i) \delta(y - x_j), \quad (3)$$

where the sum is over the set of bidirectional links and  $\mathcal{L}$  is their number. The physical units of the  $W$ s are the inverse of the volume of the space. The motivation for dividing the brain connectivity in two parts is discussed in Sec. VI and rests on the need to develop a model which incorporates data derived from human physiology.

In this paper we are interested in the perturbation to the stationary solution of Eq. (1). Writing  $\psi(x, t) = \psi_0(x) + \psi_1(x, t)$ , where  $\psi_0(x)$  is the solution satisfying  $\dot{\psi}(x, t) = 0$ , the neural field equation for the perturbation  $\psi_1(x, t)$

becomes

$$\begin{aligned} \dot{\psi}(x, t) + \epsilon \psi(x, t) &= \nu \int_{\mathcal{D}} W_{\text{hom}}(|x - y|) \psi(y, t - |x - y|/c) dy \\ &+ \nu \int_{\mathcal{D}} W_{\text{het}}(x, y) \psi(y, t - |x - y|/\nu) dy, \end{aligned} \quad (4)$$

where we relabeled  $\psi_1 \rightarrow \psi$  and  $\nu = \partial S / \partial \psi$  is a constant with the dimensions of a frequency. In deriving Eq. (4) we made the assumption that the nonhomogeneous stationary solution  $\psi_0(x)$  works in the linear domain of the sigmoid function  $S$ . More details on the derivation of Eqs. (1) and (4) can be found in Refs. [37,38,47].

### III. CIRCUMFERENCE

In this section we obtain the expression of the neural field equation on a circular spatial domain. We start considering the homogeneous connectivity term without delay, which is equivalent to the  $c \rightarrow \infty$  limit, corresponding to instantaneous signal propagation: The result is a diffusion equation with a sink term. Then we consider the homogeneous term with a finite value for  $c$ , thus introducing the effect of the delay: The result is still a diffusive equation with a sink term but the coefficients are rescaled according to a  $c$  dependence.

Finally, we analyze the full equation by adding the heterogeneous term with its delay and performing the mode decomposition. Working in the frequency domain, we obtain the exact form for the characteristic equation of (4) in a form suitable for a truncation approximation.

#### A. Instantaneous homogeneous connectivity

The starting point of our analysis is the representation

$$\psi(\theta, t) = \sum_m \xi_m(t) e^{im\theta} \quad (5)$$

for the local field potential  $\psi(\theta, t)$ . The functions  $\xi_m(t)$  are the coefficients of our mode decomposition. Working on the circumference, the natural choices for the basis functions are the complex exponentials, being  $m \in \mathbb{Z}$ . The homogeneous term of the integral in Eq. (4) for a circular domain can be written, disregarding the delay, in the following form:

$$\begin{aligned} I(\theta, t) &\equiv \nu \int_{\mathcal{C}} W_{\text{hom}}(d(\theta, \theta')) \psi(\theta', t) d\theta' \\ &= \nu \int_{\mathcal{C}} W_{\text{hom}}(d(\theta, \theta')) \sum_m \xi_m(t) e^{im\theta'} d\theta', \end{aligned} \quad (6)$$

where the integral is on the unitary circumference  $\mathcal{C} \equiv \mathbb{S}^1$  and  $d(\theta, \theta')$  is the distance between two points, the length of the shorter arc connecting the two points on the circumference. In this paper all lengths are measured in units of the circumference or sphere radius so that  $R \equiv 1$  will set the length unit.

Since  $W_{\text{hom}}$  is a fast-decaying function of the distance between two points on the circumference, we change the integration variable  $\theta'$  so that it measures the distance from the ‘‘observation’’ point  $\theta$ . This is accomplished by a rotation which, on the basis functions, acts as  $e^{im\theta'} \rightarrow e^{-im\theta} e^{im\theta'} = e^{-im\bar{\theta}}$  with  $\bar{\theta} \equiv \theta - \theta'$ . In this way the distance  $d = \cos^{-1}[\cos \bar{\theta}]$  can be

expressed as  $d = |\bar{\theta}|$  if the domain  $[-\pi, +\pi]$  is used. Assuming an exponentially decaying homogeneous connectivity, the connectivity function takes the form  $W_{\text{hom}}(\bar{\theta}) = N(\sigma) e^{-|\bar{\theta}|/\sigma}$ , where  $N(\sigma)^{-1} = \int_{-\pi}^{\pi} e^{-|\bar{\theta}|/\sigma} d\bar{\theta}$  is the normalization. Thus,

$$\begin{aligned} I(\theta, t) &= \nu N(\sigma) \sum_m \xi_m(t) e^{im\theta} \int_{-\pi}^{\pi} e^{-|\bar{\theta}|/\sigma} e^{-im\bar{\theta}} d\bar{\theta} \\ &= \nu N(\sigma) \sum_m \xi_m(t) e^{im\theta} \\ &\times \int_{-\pi}^{\pi} e^{-|\bar{\theta}|/\sigma} \left( 1 - im\bar{\theta} - \frac{m^2}{2} \bar{\theta}^2 + \dots \right) d\bar{\theta} \\ &= \nu N(\sigma) \sum_m \xi_m(t) e^{im\theta} \\ &\times \left( \frac{1}{N(\sigma)} - \frac{m^2}{2} \int_{-\pi}^{\pi} \bar{\theta}^2 e^{-|\bar{\theta}|/\sigma} + \dots \right) d\bar{\theta}, \end{aligned} \quad (7)$$

where the  $-im\bar{\theta}$  integral vanishes by symmetry. Since the second derivative of  $\psi$  with respect to  $\theta$  is represented by  $\sum_m (-m^2) \psi_m \exp(im\theta)$ , the second-order approximation reads

$$\dot{\psi}(\theta, t) + (\epsilon - \nu) \psi(\theta, t) = D \psi''(\theta, t), \quad (8)$$

where  $\psi'' \equiv \partial_{\theta\theta} \psi$  and the diffusion coefficient  $D$  is given by

$$D = \nu \frac{N(\sigma)}{2} \int_{-\pi}^{\pi} \bar{\theta}^2 e^{-|\bar{\theta}|/\sigma} d\bar{\theta}. \quad (9)$$

As already stated, this equation has the form of a diffusive equation with a sink term.

#### B. Homogeneous connectivity with delay

We now introduce a time delay in the pairwise connection, taking into account the finite velocity of transmission,  $c$ . Since the neural signal propagation encoded in  $W_{\text{hom}}$  is considered to be ‘‘fast,’’ we perform a first-order Taylor expansion in the time dependence of the neural field. Thus,

$$\begin{aligned} I(\theta, t) &= \nu \int_{-\pi}^{\pi} W_{\text{hom}}(d(\theta, \theta')) \psi(\theta', t - d(\theta, \theta')/c) d\theta' \\ &= \nu \int_{-\pi}^{\pi} W_{\text{hom}}(|\bar{\theta}|) \sum_m e^{im\theta} e^{-im\bar{\theta}} \xi_m(t - |\bar{\theta}|/c) d\bar{\theta} \\ &= \nu \sum_m e^{im\theta} \\ &\times \int_{-\pi}^{\pi} W_{\text{hom}}(|\bar{\theta}|) e^{-im\bar{\theta}} \left( \xi_m(t) - \frac{|\bar{\theta}|}{c} \partial_t \xi_m(t) + \dots \right) d\bar{\theta} \\ &= \nu \psi(\theta, t) + D \psi''(\theta, t) - \frac{\nu}{c} A \dot{\psi}(\theta, t), \end{aligned} \quad (10)$$

where

$$A = \int_{-\pi}^{\pi} |\bar{\theta}| W_{\text{hom}}(|\bar{\theta}|) d\bar{\theta} \quad (11)$$

and  $D$  is still given by Eq. (9). We conclude that, when only the homogeneous term is considered and with the introduction of the delay, the neural field equation (4) can be written as

$$\dot{\psi} + \epsilon' \psi = D' \psi'', \quad (12)$$

where

$$\epsilon' = \frac{\epsilon - v}{1 + vA/c}, \quad D' = \frac{D}{1 + vA/c}. \quad (13)$$

As already stated, we see two things: (1) the equation structure is the same as that of Eqs. (8) and (2) the introduction of a delay only redefines the coefficients  $\epsilon$  and  $D$ .

Notice that all the results obtained so far are based on the two features of the homogeneous connectivity: Its fast decaying nature, which allows for a Taylor expansion in the space variable, and its rotational invariance, which makes the  $\partial_\theta$  term vanish. Finally, the delay term results in a correction to the  $\partial_t$  term, due to the “high” value of  $c$ . All these qualitative features translate to the spherical case of Sec. IV. This means that, recalling that  $R \equiv 1$  sets the length unit and putting  $\epsilon \equiv 1$  to set the frequency and time units, all the physiological variability described by  $W_{\text{hom}}$  is encoded only into the two coefficients  $\epsilon'$  and  $D'$  through its spatial moments. It is unlikely that such a model can account for the great variability observed in EEG recordings. To make the model closer to physiological evidence, the subject-dependent heterogeneous term must be introduced in order to explore to what extent it is needed to account for such complexity.

### C. Heterogeneous connectivity

We now consider the heterogeneous term which contains the long-range connectivity. The aim of this section is to write the neural field equation in a form suitable for a truncation expansion on the relevant eigenmodes. We see that the final form can be divided in part related to the topology of the physical space and in part related to the neuronal connectivity and the delay.

First of all we note that in Eqs. (1) and (4) the function  $W_{\text{het}}$  is a continuous function of two variables but in Eq. (3) we consider, as a significant example, a  $\delta$ -shaped connectivity with link strengths given by  $\mu_{ij}$ . Since the following treatment is as general as possible, we still use a continuous representation for the heterogeneous connectivity but, having in mind the discontinuous ( $\delta$ -like) form of Eq. (3), we change notation from  $W_{\text{het}}(x, y)$  to  $\mu(x, y)$ , representing it in a continuous fashion. Because  $\mu(x, y)$  is related to the long-range connections, we cannot assume a particular parametrization, as we have done for  $W_{\text{hom}}$ , nor we can suppose it is a monotonic function of its spatial variables.

In order to perform the mode decomposition, we substitute representation (5) into Eq. (4). Then we approximate the homogeneous term with its first nontrivial Taylor expansions, according to the procedure of Secs. III A and III B. Finally, we project on the basis functions. The result is

$$\dot{\xi}_m(t) = -(\epsilon + Dm^2)\xi_m(t) + \mathcal{I}(t, m), \quad (14)$$

$$\begin{aligned} \mathcal{I}(t, m) \equiv & \int_{\theta_1} \int_{\theta_2} \mu(\theta_1, \theta_2) e^{-im\theta_1} \\ & \times \sum_n e^{in\theta_2} \xi_n(t - d(\theta_1, \theta_2)/v) d\theta_1 d\theta_2. \end{aligned} \quad (15)$$

In Eq. (14) the quantities  $\epsilon$  and  $D$  are the rescaled ones of Eq. (13) while in Eq. (15) we have  $\mu(\theta_1, \theta_2) \equiv W_{\text{het}}/A$  with  $A$  given by Eq. (11). These equations are exact, apart from

the short-range and high- $c$  approximations on  $W_{\text{hom}}$  already discussed. We now proceed to work on the heterogeneous integral (15). We take three steps:

(i) Expand the heterogeneous connectivity on the basis of complex exponentials as  $\mu(\theta_1, \theta_2) = \sum_{m_1, m_2} \mu_{m_1, m_2} e^{im_1\theta_1} e^{im_2\theta_2}$ . In the following discussion a number of  $\pi$  factors arise since we have used the non-normalized  $e^{im\theta}$  basis functions.

(ii) Change variable  $\theta_2 \rightarrow \bar{\theta}$  through a rotation so that  $|\bar{\theta}| = d(\theta_1, \theta_2)$  with  $\bar{\theta} \in [-\pi, \pi]$  and relabel  $\theta \equiv \theta_1$ .

(iii) Fourier transform in the time domain the  $\xi_n(t)$  coefficients.

A comment is in order about step (i). The expansion for  $\mu$  is an exact representation as long as the sums involve infinite terms. This means that a connectivity of  $\delta$  links is continuously represented in an exact way but, when truncating the sums, it is smoothed, and thus approximated, to a proper continuous function.

After step (ii) we get

$$\begin{aligned} \mathcal{I}(t, m) = & \sum_{m_1, m_2} \sum_n \mu_{m_1, m_2} \\ & \times \int_{\theta} e^{i\theta(m_1+m_2-m+n)} d\theta \int_{\bar{\theta}} e^{-i\bar{\theta}(m_2+n)} \xi_m(t - |\bar{\theta}|/v) d\bar{\theta}. \end{aligned}$$

The change of variables has divided the double integral into a part which depends only on the basis functions and a part which retains the delay term. Anyway, the two factors are entangled by the sums over the modes which involve the connectivity components. It is easy to recognize that the form of the first part is dictated only by the topology of the space. Thus, we set

$$\mathcal{T} \equiv \int_{-\pi}^{\pi} e^{i\theta(m_1+m_2-m+n)} d\theta = 2\pi \delta_{m, m_1+m_2+n}. \quad (16)$$

The meaning of this equation, an expression of angular momentum conservation, is a topology constraint on the connectivity modes that can contribute to the time evolution of the  $m$ th eigenmode.

Performing the Fourier transform of step (iii), we get

$$\begin{aligned} \hat{\mathcal{I}}(\omega, m) = & \sum_{m_1, m_2} \mu_{m_1, m_2} \sum_n \hat{\xi}_n(\omega) \mathcal{T}(m, m_1, m_2, n) \\ & \times \int_{\bar{\theta}} e^{-i\bar{\theta}(m_2+n)} e^{i\omega|\bar{\theta}|/v} d\bar{\theta}. \end{aligned} \quad (17)$$

The structure of this expression is of the form

$$\begin{aligned} \hat{\mathcal{I}}(\omega, m) = & \sum_n \sum_{m_1, m_2} \mathcal{T}(m, m_1, m_2, n) \\ & \times \mathcal{W}(\omega, m_2, n) \mu_{m_1, m_2} \hat{\xi}_n(\omega), \end{aligned} \quad (18)$$

where

$$\mathcal{W} \equiv \int_{-\pi}^{\pi} e^{-i\bar{\theta}(m_2+n)} e^{i\omega|\bar{\theta}|/v} d\bar{\theta}. \quad (19)$$

Putting together all the pieces, the neural field equation in the frequency domain expanded on the complex exponentials

basis is

$$(\epsilon + m^2 D - i\omega)\hat{\xi}_m(\omega) = \sum_n \sum_{m_1, m_2} \mathcal{T}(m, m_1, m_2, n) \mathcal{W}(\omega, m_2, n) \mu_{m_1, m_2} \hat{\xi}_n(\omega) \quad (20)$$

$$= 2\pi \sum_n \sum_{m_2} \mathcal{W}(\omega, m_2, n) \mu_{m-n, m_2} \hat{\xi}_n(\omega). \quad (21)$$

In this form, the first sum is a series expansion for the  $\hat{\xi}$  coefficients, which becomes our truncation approximation, while the second sum is a ‘‘convolution-like’’ term, which cannot be further simplified without some assumption on the heterogeneous connectivity. As a consistency check, we consider the  $v \rightarrow \infty$  limit:  $\mathcal{W}(m_2, n) = 2\pi \delta_{m_2, -n} \implies \mathcal{I} = (2\pi)^2 \sum_n \mu_{m, -n} \hat{\xi}_n$ . This is the correct result that one would have gotten starting directly from  $\mathcal{I}$  without the delay. Notice that, following a standard analysis [37,48], Eqs. (20) and (21) can be easily cast into the form of a characteristic equation:

$$\mathbb{M} \cdot \xi(\omega) = 0, \quad \mathbb{M} = \mathbb{D} + \mathbb{K}, \quad (22)$$

$$\mathbb{D}_{m,n} = (\epsilon + m^2 D - i\omega) \delta_{m,n}, \quad (23)$$

$$\mathbb{K}_{m,n} = -2\pi \sum_{m_2} \mathcal{W}(\omega, m_2, n) \mu_{m-n, m_2}, \quad (24)$$

where  $\mathbb{D}$  is a diagonal matrix related to the short-range connectivity and  $\mathbb{K}$  is the matrix related to the heterogeneous kernel. In the absence of the global connectivity, this would reduce to a standard dispersion relation  $\epsilon + m^2 D - i\omega = 0$ , where for each ‘‘wavelength’’  $m$  a solution with a precise complex frequency exists. For a nonzero  $\mu$  we have instead the condition  $\det[\mathbb{M}] = 0$ , which constrains the possible values of the eigenfrequency  $\omega$ , introducing a strong ‘‘interaction’’ among all the  $m$ s.

#### IV. SPHERE

In this section we consider the neural field equation (4) on a spherical spatial domain. As we have done for the circumference, we start by assuming an instantaneous homogeneous connectivity, then we add a delay (through the parameter  $c$ ) and finally we analyze the full equation including the heterogeneous term and its delay (through the parameter  $v$ ). The analyses closely follow the ones already done for the circumference and much of the physical considerations done in Sec. III are extended to the more physical case of the sphere.

Our first result is the approximation of the homogeneous integral with the delay again through a diffusive equation with a sink term and the computation of the corresponding coefficients in terms of the spherical  $W_{\text{hom}}$ . The final result is a mode decomposition of the full field equation on the spherical harmonic basis in a form suitable for a truncation approximation.

##### A. Instantaneous homogeneous connectivity

The starting point of our analysis is now the representation for the local field potential  $\psi(\theta, \phi, t)$  on the spherical

harmonics:

$$\psi(\theta, \phi, t) = \sum_{l,m} \xi_{l,m}(t) Y_{l,m}(\theta, \phi), \quad (25)$$

where  $\theta$  and  $\phi$  are respectively the polar and azimuthal angles parametrizing the unitary sphere  $\mathcal{S} \equiv \mathcal{S}^2$ . The sums run over  $l = 0, 1, 2, \dots$  and, for each  $l$ , over  $m = -l, -l + 1, \dots, 0, \dots, l - 1, l$ . The spherical harmonics are defined as follows:

$$Y_{l,m}(\theta, \phi) = \mathcal{N}_{l,m} P_l^m(\cos \theta) e^{im\phi}, \quad (26)$$

where  $P_l^m(x)$  are the associated Legendre polynomials of order  $l$  and degree  $m$  while  $\mathcal{N}_{l,m}$  are proper normalization factors, defined by the condition  $\int_0^{2\pi} d\phi \int_0^\pi d\theta \sin \theta Y_{l,m}(\theta, \phi) = 1$ . In our conventions we have  $Y_{l,-m} = (-1)^m Y_{l,m}^*$ . It is well known that the spherical harmonics  $Y_{l,m}(\theta, \phi)$  constitute a complete and orthonormal set of functions for a spherical domain. Since our field equation involving the homogeneous connectivity is a diffusive one, spherical harmonics are the natural expansion basis, being eigenfunctions of the Laplacian operator [49]. We now study the homogeneous term of Eq. (4) in the instantaneous approximation:

$$\begin{aligned} I(\theta, \phi, t) &= v \int_{\Omega'} W_{\text{hom}}(d(\Omega, \Omega')) \psi(\Omega', t) d\Omega' \\ &= v \int_{\Omega'} W_{\text{hom}}(d(\Omega, \Omega')) \sum_{l,m} \xi_{l,m}(t) Y_{l,m}(\Omega') d\Omega', \end{aligned} \quad (27)$$

where  $\Omega \equiv (\theta, \phi)$ . Since the connectivity function has a simple form in a spherical system whose polar axis is along the direction of  $(\theta, \phi)$  [in this section the function  $d(\Omega, \Omega')$  is defined as the great circle distance between two points], we need to perform the rotation

$$Y_{l,m}(\bar{\Omega}) = \sum_{m'} D_{m',m}^{(l)}(R(\Omega)) Y_{l,m'}(\Omega'), \quad (28)$$

where  $R(\Omega) \equiv R(\alpha = \phi, \beta = \theta, \gamma = 0)$  is the rotation, parametrized through the Euler angles  $(\alpha, \beta, \gamma)$ , that actively takes the polar axis in the wanted direction.

We used the Wigner rotation matrices  $D^{(l)}$  with integer  $l$ , well known from the theory of angular momentum in quantum mechanics, since they realize the representation of the rotation group in the space of spherical harmonics which is exactly what we need to perform the change of integration variables  $\Omega' \rightarrow \bar{\Omega}$ . Wigner matrices, being a unitary representation of rotations, satisfy the following properties [49]:

$$D_{m',m}^{(l)}(R)^{-1} = D_{m',m}^{(l)\dagger}(R) = D_{m,m'}^{(l)*}(R). \quad (29)$$

Using Eq. (29) to invert Eq. (28) and substituting in Eq. (27), the integral  $I(\theta, \phi, t)$  becomes

$$\begin{aligned} I(\theta, \phi, t) &= v N(\sigma) \sum_{l,m} \xi_{l,m}(t) \\ &\quad \times \sum_{m'} D_{m',m}^{(l)}(R(\Omega))^{-1} \int_{\bar{\Omega}} e^{-\bar{\theta}/\sigma} Y_{l,m'}(\bar{\Omega}) d\bar{\Omega} \\ &= v N(\sigma) \sum_{l,m} \xi_{l,m}(t) D_{0,m}^{(l)}(R(\Omega))^{-1} \int_{\bar{\Omega}} e^{-\bar{\theta}/\sigma} Y_{l,0}(\bar{\Omega}) d\bar{\Omega} \end{aligned}$$

$$= \nu N(\sigma) \sum_{l,m} \xi_{l,m}(t) \times \sqrt{\frac{4\pi}{2l+1}} Y_{l,m}(\theta, \phi) \int_{\bar{\Omega}} e^{-\bar{\theta}/\sigma} Y_{l,0}(\bar{\Omega}) d\bar{\Omega}, \quad (30)$$

where  $N$  is the proper normalization for the homogeneous connectivity on the sphere. In the first passage the resulting integral does not depend on  $\bar{\phi}$  so that only the  $m' = 0$  terms remain while in the last passage we used the relation [49]

$$D_{m,0}^{(l)}(\phi, \theta, \gamma) = \sqrt{\frac{4\pi}{2l+1}} Y_{l,m}^*(\theta, \phi) \rightarrow D_{0,m}^{(l)}(R^{-1}(\Omega)) = \sqrt{\frac{4\pi}{2l+1}} Y_{l,m}(\theta, \phi). \quad (31)$$

Assuming again a fast-decaying connectivity function, we use the Taylor expansion, about  $\theta = 0$ ,  $\phi = 0$ , for the spherical harmonics inside the integral to get the second-order approximation as

$$I(\theta, \phi, t) = \nu N(\sigma) \sum_{l,m} \xi_{l,m}(t) Y_{l,m}(\theta, \phi) \sqrt{\frac{4\pi}{2l+1}} \times \int_{\bar{\Omega}} \left( Y_{l,0}(0, 0) + \frac{\partial Y_{l,0}}{\partial \bar{\theta}}(0, 0) \bar{\theta} + \frac{1}{2} \frac{\partial^2 Y_{l,0}}{\partial \bar{\theta}^2}(0, 0) \bar{\theta}^2 \right) e^{-\bar{\theta}/\sigma} d\bar{\Omega}, \quad (32)$$

where  $\partial_{\phi} Y_{l,0} = 0$  has been used so that all the azimuthal derivatives vanish. We need the values of the derivatives with respect to the polar angle of the spherical functions with  $m = 0$  at the north pole: The results are  $\partial_{\theta} Y_{l,0}(0, 0) = 0$  and  $\partial_{\theta}^2 Y_{l,0}(0, 0) = -\frac{1}{2} l(l+1) Y_{l,0}(0, 0)$ .

Substituting in the integral, we finally get

$$I(\theta, \phi, t) = \nu \psi(\theta, \phi, t) - \sum_{l,m} l(l+1) \xi_{l,m}(t) \times Y_{l,m}(\theta, \phi) \nu \frac{N(\sigma)}{4} \int_{\bar{\Omega}} \bar{\theta}^2 e^{-\bar{\theta}/\sigma} d\bar{\Omega}, \quad (33)$$

where  $Y_{l,0}(0, 0) = \sqrt{(2l+1)/4\pi} P_l(1) = \sqrt{(2l+1)/4\pi}$  has been used.

We see that we obtained the representation of the Laplacian operator on the unit sphere and thus the homogeneous part of the neural field equation can be rewritten as

$$\dot{\psi}(\theta, \phi, t) + (\epsilon - \nu) \psi(\theta, \phi, t) = D \nabla^2 \psi(\theta, \phi, t), \quad (34)$$

where the diffusion coefficient is given by

$$D = \nu \frac{N(\sigma)}{4} \int_{\bar{\Omega}} \bar{\theta}^2 e^{-\bar{\theta}/\sigma} d\bar{\Omega}. \quad (35)$$

Also for the spherical domain the resulting equation is a diffusive equation with a sink term.

### B. Homogeneous connectivity with delay

We take advantage of the preceding results to study the homogeneous term with a delay. Introducing the time delay in the homogeneous integral (27) through the parameter  $c$  and

using the result (30), we can take a Taylor expansion of  $\xi_{l,m}(t)$ :

$$I(\theta, \phi, t) = \nu \int_{\Omega'} W_{\text{hom}}(d(\Omega, \Omega')) \psi(\Omega', t - d(\Omega, \Omega')/c) d\Omega' = \nu N(\sigma) \sum_{l,m} \sqrt{\frac{4\pi}{2l+1}} Y_{l,m}(\theta, \phi) \times \int_{\bar{\Omega}} \xi_{l,m}(t - \bar{\theta}/c) e^{-\bar{\theta}/\sigma} Y_{l,0}(\bar{\Omega}) d\bar{\Omega} = \nu N(\sigma) \sum_{l,m} \sqrt{\frac{4\pi}{2l+1}} Y_{l,m}(\theta, \phi) \times \int_{\bar{\Omega}} \left( \xi_{l,m}(t) - \frac{\bar{\theta}}{c} \partial_t \xi_{l,m}(t) + \dots \right) e^{-\bar{\theta}/\sigma} Y_{l,0}(\bar{\Omega}) d\bar{\Omega} = \nu \psi(\theta, t) + D \nabla^2 \psi(\Omega, t) - \frac{\nu}{c} B \dot{\psi}(\theta, t), \quad (36)$$

where now

$$B = N(\sigma) \int_{\bar{\Omega}} \bar{\theta} e^{-\bar{\theta}/\sigma} d\bar{\Omega} \quad (37)$$

is the analogy of the circumference coefficient  $A$  of Eq. (11). Recalling the starting field equation  $\dot{\psi} + \epsilon \psi = I$ , we get

$$\dot{\psi} + \frac{\epsilon - \nu}{1 + \nu B/c} \psi = \frac{D}{1 + \nu B/c} \nabla^2 \psi \quad (38)$$

so that we can again read the new decaying constant  $\epsilon'$  and diffusion coefficient  $D'$ :

$$\epsilon' = \frac{\epsilon - \nu}{1 + \nu B/c}, \quad D' = \frac{D}{1 + \nu B/c}. \quad (39)$$

The structure of the equation is again a diffusion equation with a sink term where the coefficients are given in terms of opportune moments of the function  $W_{\text{hom}}$  and renormalized by the delay term.

### C. Heterogeneous connectivity

We now consider the full field equation (4) on the spherical domain. According to the discussion of Sec. II and the analysis of Sec. III, we get our starting point in the form

$$\dot{\xi}_{l,m}(t) = -(\epsilon + Dl(l+1)) \xi_{l,m}(t) + \mathcal{I}(t, l, m), \quad (40)$$

$$\mathcal{I}(t, l, m) \equiv \int_{\Omega_1} \int_{\Omega_2} \mu(\Omega_1, \Omega_2) Y_{lm}^*(\Omega_1) \times \sum_{l'm'} Y_{l'm'}(\Omega_2) \xi_{l'm'}(t - d(\Omega_1, \Omega_2)/\nu) d\Omega_1 d\Omega_2, \quad (41)$$

where  $\epsilon$  and  $D$  are given by Eq. (39) but now  $\mu \equiv W_{\text{het}}/B$  with  $B$  given by Eq. (37). We perform the analogy of the three steps already taken for the circumference:

(1) Expand the heterogeneous connectivity on the spherical harmonic basis.

(2) Change variable  $\Omega_2 \rightarrow \bar{\Omega}$  through a rotation so that  $\bar{\theta} = d(\theta_1, \theta_2)$  and relabel  $\Omega \equiv \Omega_1$ .

(3) Fourier transform in the time domain the  $\xi_{l,m}(t)$  coefficients.

The final result is

$$\begin{aligned} \hat{\mathcal{I}}(\omega, l, m) &= \int_{\Omega} \int_{\bar{\Omega}} \sum_{l_1, m_1} \sum_{l_2, m_2} \mu_{l_1, m_1, l_2, m_2} Y_{l, m}^*(\Omega) Y_{l_1, m_1}(\Omega) \\ &\times \sum_{l', m'} \sum_{m'_2, m''} \hat{\xi}_{l', m'}(\omega) \\ &\times D_{m'_2, m_2}^{(l_2)}(R^{-1}(\Omega)) D_{m', m'}^{(l')}(R^{-1}(\Omega)) \\ &\times Y_{l_2, m'_2}(\bar{\Omega}) Y_{l', m''}(\bar{\Omega}) e^{i\omega\bar{\theta}/v} d\Omega d\bar{\Omega}. \end{aligned} \quad (42)$$

Using the properties (29) for  $D^{(l)}(R^{-1})$  and  $D_{m', m}^{(l)*}(R) = (-1)^{m'-m} D_{-m', -m}^{(l)}(R)$ , we can rewrite the last equation as

$$\begin{aligned} \hat{\mathcal{I}}(\omega, l, m) &= \int_{\Omega} \int_{\bar{\Omega}} d\Omega d\bar{\Omega} \sum_{l_1, m_1} \sum_{l_2, m_2} \mu_{l_1, m_1, l_2, m_2} (-1)^m \\ &\times Y_{l, -m}(\Omega) Y_{l_1, m_1}(\Omega) \sum_{l', m'} \sum_{m'_2, m''} \hat{\xi}_{l', m'}(\omega) \\ &\times (-1)^{m'+m_2-m''-m'_2} D_{-m_2, -m'_2}^{(l_2)}(R(\Omega)) D_{-m', -m''}^{(l')}(R(\Omega)) \\ &\times (R(\Omega)) Y_{l_2, m'_2}(\bar{\Omega}) Y_{l', m''}(\bar{\Omega}) e^{i\omega\bar{\theta}/v}. \end{aligned} \quad (43)$$

Once again in the spherical case, we recognize a factorization over the integration variables which identifies a topology-related part  $\mathcal{T}$  and a delay-related part  $\mathcal{W}$ :

$$\begin{aligned} \mathcal{T} &= (-1)^{m+m'+m_2-m''-m'_2} \int_{\Omega} Y_{l, -m}(\Omega) Y_{l_1, m_1}(\Omega) \\ &\times D_{-m_2, -m'_2}^{(l_2)}(R(\Omega)) D_{-m', -m''}^{(l')}(R(\Omega)) d\Omega, \end{aligned} \quad (44)$$

$$\mathcal{W} = \int_{\bar{\Omega}} Y_{l_2, m'_2}(\bar{\Omega}) Y_{l', m''}(\bar{\Omega}) e^{i\omega\bar{\theta}/v} d\bar{\Omega}. \quad (45)$$

In order to study the topology function, we first write the product of the two spherical harmonics as a Clebsch-Gordan series:

$$\begin{aligned} Y_{l, -m}(\Omega) Y_{l_1, m_1}(\Omega) \\ = \sum_{L, M} \sqrt{\frac{(2l+1)(2l_1+1)}{4\pi(2L+1)}} C_{l, 0, l_1, 0}^{L, 0} C_{l, -m, l_1, m_1}^{L, M} Y_{L, M}(\Omega), \end{aligned} \quad (46)$$

where  $L$  satisfies the triangular rule  $|l - l_1| \leq L \leq l + l_1$  and we use the Condon-Shortley convention for the phases of the Clebsch-Gordan coefficients, so that they are real. Then we use relation (31) to convert a spherical harmonic function into the proper element of a Wigner matrix and we get

$$\begin{aligned} \mathcal{T} &= (-1)^{m+m'+m_2-m''-m'_2} \sum_{L, M} \frac{\sqrt{(2l+1)(2l_1+1)}}{4\pi} \\ &\times C_{l, 0, l_1, 0}^{L, 0} C_{l, -m, l_1, m_1}^{L, M} \\ &\times \int_{\Omega} D_{M, 0}^{(L)*}(R(\Omega)) \times D_{-m_2, -m'_2}^{(l_2)}(R(\Omega)) \\ &\times D_{-m', -m''}^{(l')}(R(\Omega)) d\Omega. \end{aligned} \quad (47)$$

Noting that the rotation involved in the  $\Omega$  integral, in terms of Euler angles, is  $R(\phi, \theta, 0)$ , it is possible to use the orthonormality relation of the Wigner matrices for the special

case of axial symmetry:

$$\begin{aligned} \int_{\Omega} D_{M', M}^{(L)*}(\phi, \theta, 0) D_{m'_1, m_1}^{(l_1)}(\phi, \theta, 0) D_{m'_2, m_2}^{(l_2)}(\phi, \theta, 0) d\Omega \\ = \frac{4\pi}{2L+1} C_{l_1, m_1, l_2, m_2}^{L, M} C_{l_1, m'_1, l_2, m'_2}^{L, M'}. \end{aligned} \quad (48)$$

For  $\mathcal{T}$  we thus obtain

$$\begin{aligned} \mathcal{T} &= (-1)^{m+m'+m_2-m''-m'_2} \sum_{L, M} \frac{\sqrt{(2l+1)(2l_1+1)}}{2L+1} \\ &\times C_{l, 0, l_1, 0}^{L, 0} C_{l, -m, l_1, m_1}^{L, M} C_{l_2, -m'_2, l', -m''}^{L, 0} C_{l_2, -m_2, l', -m'}^{L, M}. \end{aligned} \quad (49)$$

To proceed further, we extract from the Clebsch-Gordan coefficients the constraints for the azimuthal quantum numbers:  $m'' + m'_2 = 0$  and  $m = m_1 + m_2 + m'$ . A comment is in order: We see that the integral in  $\mathcal{W}$  is nonzero only for  $m'_2 = -m''$ , which is consistent with the constraint already given by the  $\mathcal{T}$  term. Of course this is a consequence of the fact that the time delay depends only on the distance of  $\Omega_1$  and  $\Omega_2$ . Finally, putting together all the results, we have our final expansion for the topology function:

$$\begin{aligned} \mathcal{T} &= (-1)^{m_1} \sum_L \frac{\sqrt{(2l+1)(2l_1+1)}}{2L+1} \\ &\times C_{l, 0, l_1, 0}^{L, 0} C_{l_2, m'', l', -m''}^{L, 0} C_{l, -m, l_1, m_1}^{L, m_1-m} C_{l_2, m_1+m'-m, l', -m'}^{L, m_1-m}. \end{aligned} \quad (50)$$

Working in the frequency domain, as already noted in the study of the circumference, we can recast our results in the form of a characteristic equation:

$$\mathbb{M} \cdot \xi(\omega) = 0, \quad \mathbb{M} = \mathbb{D} + \mathbb{K}, \quad (51)$$

$$\mathbb{D}_{lm, l'm'} = (\epsilon + l(l+1)D - i\omega) \delta_{lm, l'm'} \quad (52)$$

$$\begin{aligned} \mathbb{K}_{lm, l'm'} &= \sum_{l_1, m_1} \sum_{l_2, m_2} \sum_{m'_2, m''} \mathcal{T}(lm; l'm'; l_1 m_1; l_2 m_2; m'_2 m'') \\ &\times \mathcal{W}(\omega; l_2 m'_2; l' m'') \mu_{l_1, m_1, l_2, m_2}, \end{aligned} \quad (53)$$

where  $\mathbb{D}$  is a diagonal matrix related to the homogeneous part of the model and  $\mathbb{K}$  is the matrix related to the heterogeneous kernel. Once again  $\det[\mathbb{M}] = 0$  is the characteristic equation which now identifies the eigenfrequency  $\omega$  which describes the intricate “interactions” of the modes  $l, m$ .

## V. PRINCIPAL RESULTS

Here we want to stress the principal results of our work. Our final result for the Fourier transforms  $\hat{\xi}_{l, m}(\omega)$  is

$$\begin{aligned} (\epsilon + D l(l+1) - i\omega) \hat{\xi}_{l, m}(\omega) \\ = \sum_{l', m'} \hat{\xi}_{l', m'}(\omega) \sum_{l_1, m_1} \sum_{l_2} \mu_{l_1, m_1, l_2, m_1+m'-m} \\ \times \sum_{m''} \mathcal{T}(lm; l'm'; l_1 m_1; l_2 m'') \mathcal{W}(\omega, l', l_2, m''), \end{aligned} \quad (54)$$

where the coefficients  $\epsilon$  and  $D$  given in Eq. (39) are related to the spatial moments of homogeneous connectivity while the  $\mu$  components are related to the heterogeneous connectivity. The functions  $\mathcal{T}$  and  $\mathcal{W}$  are defined in Eqs. (50) and (45)

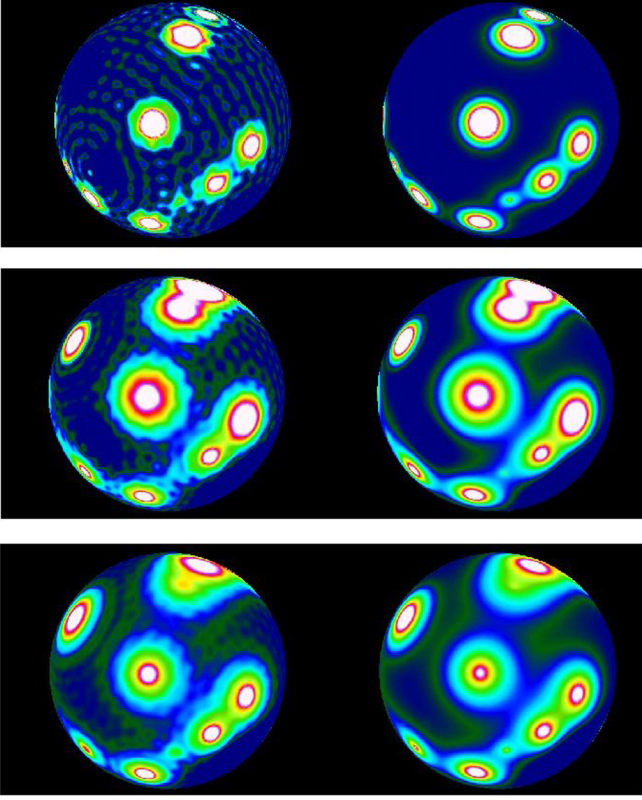


FIG. 1. 3D visualization of the neural field simulated on an inflated hemisphere using a  $34 \times 34$  weight matrix [50]; 132 608 neural populations have been simulated, and three successive time steps are shown (time increases from top to bottom). The data have been processed using MRTRIX3 and FREESURFER. Every image shows two spheres: On the left, the neural field obtained with a mode decomposition ( $l_{\max} = 50$ ) is represented; on the right, the neural field has been obtained with a finite volume method. All the figures share the same color scale, where white is high value and black is low. The weight matrix is antisymmetric, and the parameters have been chosen so that the system falls into an oscillatory regime ( $\epsilon = 0.1$ ,  $v = 0.1$ ,  $D = 0.01$ , maximum delay 20; unit of measure for time is milliseconds, and unit of measure for space is the radius of the sphere).

and represent the effect of the space topology and the delay, respectively.

The time evolution of the projection of the neural field onto the eigenfunctions of the Laplacian operator, respectively on the circumference and on the sphere, is described by the following equations:

$$\begin{aligned} \dot{\xi}_m(t) &= -(\epsilon + m^2 D)\xi_m(t) \\ &+ \sum_{ij}^{\mathcal{L}} \mu_{ij} e^{-im\theta_i} \sum_n e^{in\theta_j} \xi_n(t - d_{ij}/v), \quad (55) \\ \dot{\xi}_{l,m}(t) &= -(\epsilon + l(l+1)D)\xi_{l,m}(t) \\ &+ \sum_{ij}^{\mathcal{L}} \mu_{ij} Y_{l,m}^*(\Omega_i) \sum_{l',m'} Y_{l',m'}(\Omega_j) \xi_{l',m'}(t - d_{ij}/v). \quad (56) \end{aligned}$$

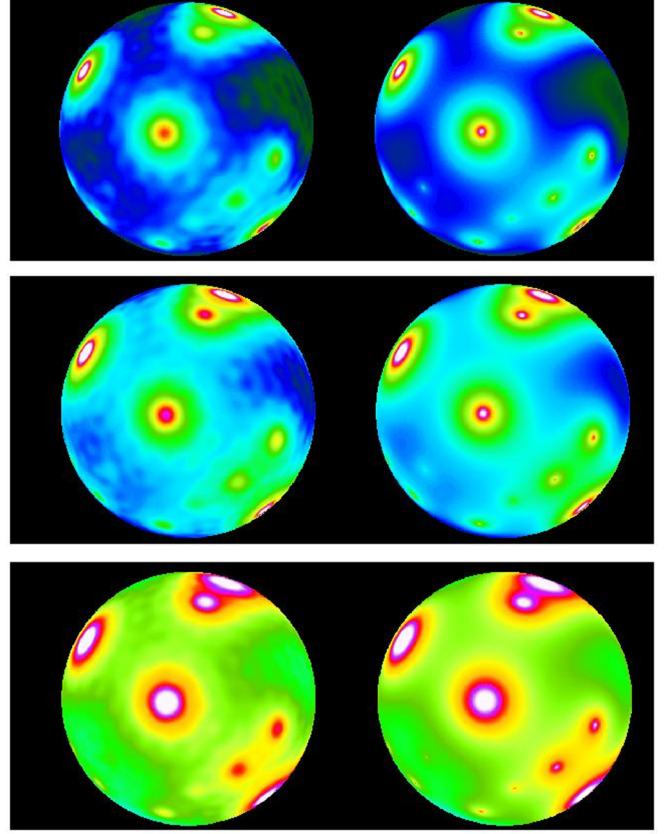


FIG. 2. 3D visualization of the neural field simulated under the same conditions as Fig. 1, but with the weight matrix that has only positive elements and  $D = 0.001$ . In this case, the system reaches a stationary state (fixed point).

Notice that the equations for the mode coefficients have the form of a dissipative process.

The dissipation becomes stronger for higher-order modes, thus suggesting that a truncation of the series might produce a

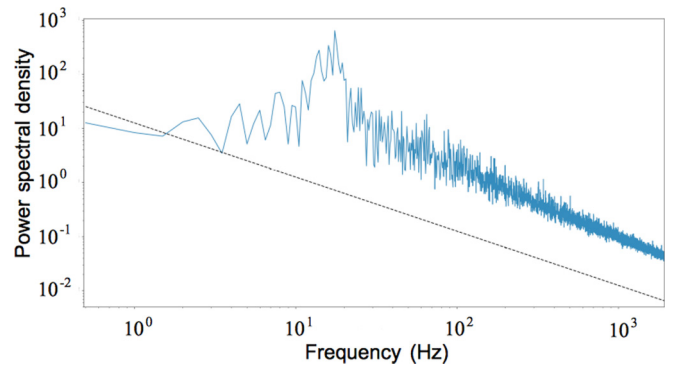


FIG. 3. Power spectral density of the neural field obtained by introducing noise into Eq. (56) via a Wiener process with variance 0.045 and amplitude 5. The parameters have been chosen so that the state of the system fluctuates around a fixed point ( $\epsilon = 0.1$ ,  $v = 0.1$ ,  $D = 0.1$ ), but it is near to bifurcate to the limit-cycle regime: The expected peak is clearly visible. A single heterogeneous connection is present, and the weight matrix  $\mu_{ij}$  is antisymmetric (this condition maximizes the amplitude of the peak). The dashed line represents a  $y \propto 1/f^2$ , which is the behavior seen for purely homogeneous connectivity.



reliable approximated solution. We illustrate this in Figs. 1 and 2, where a three-dimensional (3D) visualization of the neural field calculated onto a sphere is shown both for the (truncated) mode decomposition and the numerical evaluation (through the finite volume method) of the neural field equation. From a qualitative comparison, it is possible to see that the mode decomposition is capable of capturing the correct dynamics features of the nonapproximated solution, with a spatial resolution that is related to the  $l$  that is chosen for the truncation.

In Fig. 3, the power spectral density (PSD) of the resting state of the noise-driven neural field sources on the sphere is shown, mimicking the one-dimensional result shown in Ref. [36]. This result has been obtained using the mode decomposed equation (56) with  $l_{\max} = 20$ ; the model is still able to capture the peak typically shown in the PSD of EEG data (shown, for example, in Ref. [36]).

## VI. SUMMARY AND DISCUSSION

In recent years, experimental techniques in measuring neuroanatomical properties of the brain cortex made it possible to study neural field models where connectivities are no longer modeled in a generic fashion but can be introduced explicitly as specific inputs from individual brain imaging data. Along this line of research, in Ref. [36] Jirsa studied a one-dimensional model in a linear spatial domain with a toy connectome of one bidirectional connection and established a linear stability analysis of the dynamics and analyses of power-spectra features. The complexity of the model lies in the space-time structure of the connectome, which expresses itself, once reduced via mode decompositions, through a finite set of delay-differential equations (after truncation). Since our aim has been to go a step further towards a realistic description of the cerebral cortex, we have considered the same model in the domain of a spherical surface and retained a general connectivity. We thus performed an expansion on the spherical harmonic basis in order to get the equations for the corresponding coefficients  $\xi_{l,m}(t)$ . Working in the frequency domain, the field equation is turned into a characteristic equation

among  $\omega$  and the coefficients  $l, m$ . Despite the mathematical complexity of our result [Eq. (54)], it is exact, apart from the Taylor approximation of  $W_{\text{hom}}$ .

Considering the complex time evolution of the neural fields with time delays, we use the equations for the mode coefficients [Eqs. (14) and (15)] for the circumference and Eqs. (40) and (41) for the sphere, respectively. We render the equations specific to the connectivity in Eq. (3).

The corticocortical time delays introduce resonant behaviors characteristic of the so-called space-time structure of connectivity (see Refs. [36,51,52]) and enable selectivity of spatiotemporal behaviors due to connectivity changes and delay changes. The latter is significantly less common in the literature, but prevalent in oscillatory behaviors. Another important source of resonances is the corticothalamic, which represents a more complex type of local dynamics, since it introduces an effective time delay to all cortical regions, communicated through the thalamus [53]. The corticothalamic loop has proven to be explanatory for a wide range of resonances and dynamic behaviors [39,53,54].

In the spatial domain, the presence of time delays due to the heterogeneous connectivity term leads to high memory and time usage. Solving the truncated equations of the mode coefficients space removes this limitation and provides an important contribution to the solving of high-dimensional connectome-based brain network models. Moreover, the truncated equations provide analytical results like Eq. (54), which now allow the explicit treatment of more biologically realistic scenarios (for instance inclusion of shot noise [55], plasticity [56], and multiscale architectures [14]) that were tangible so far only under strong approximations.

## ACKNOWLEDGMENTS

This research has been partially supported by the European Union's Horizon 2020 Framework Programme for Research and Innovation under the Specific Grant Agreements No. 720270 (HBP SGA1) and No. 785907 (HBP SGA2) and the grant "PANACEE" (Prevision and analysis of brain activity in transitions: Epilepsy and sleep) of the Regione Toscana - PAR FAS 2007-2013 1.1.a.1.1.2 - B22I14000770002.

- 
- [1] A. V. M. Herz, T. Gollisch, C. K. Machens, and D. Jaeger, Modeling single-neuron dynamics and computations: A balance of detail and abstraction, *Science* **314**, 80 (2006).
  - [2] W. Gerstner, H. Sprekeler, and G. Deco, Theory and simulation in neuroscience, *Science* **338**, 60 (2012).
  - [3] G. B. Ermentrout and D. H. Terman, *Mathematical Foundations of Neuroscience* (Springer, London, 2010).
  - [4] W. Gerstner, W. M. Kistler, R. Naud, and L. Paninski, *Neuronal Dynamics: From Single Neurons to Networks and Models of Cognition* (Cambridge University Press, Cambridge, UK, 2014).
  - [5] R. D. Traub, D. Contreras, M. O. Cunningham, H. Murray, F. E. LeBeau, A. Roopun, A. Bibbig, W. B. Wilent, M. J. Higley, and M. A. Whittington, Single-column thalamocortical network model exhibiting gamma oscillations, sleep spindles, and epileptogenic bursts, *J. Neurophysiol.* **93**, 2194 (2005).
  - [6] H. Markram, The blue brain project, *Nat. Rev. Neurosci.* **7**, 153 (2006).
  - [7] E. M. Izhikevich and G. M. Edelman, Large-scale model of mammalian thalamocortical systems, *Proc. Natl. Acad. Sci. USA* **105**, 3593 (2008).
  - [8] W. J. Freeman, *Mass Action in the Nervous System. Examination of the Neurophysiological Basis of Adaptive Behavior through the EEG* (Academic Press, London, 1975).
  - [9] P. L. Nunez, The brain wave equation: A model for the EEG, *Math. Biosci.* **21**, 279 (1974).
  - [10] H. R. Wilson and J. D. Cowan, Excitatory and inhibitory interactions in localized populations of model neurons, *Biophys. J.* **12**, 1 (1972).

- [11] H. R. Wilson, and J. D. Cowan, A mathematical theory of the functional dynamics of cortical and thalamic nervous tissue, *Kybern.* **13**, 55 (1973).
- [12] S. Amari, Homogeneous nets of neuron-like elements, *Biol. Cybernetics* **17**, 211 (1975).
- [13] S. Amari, Dynamics of pattern formation in lateral-inhibition type neural fields, *Biol. Cybernetics* **27**, 77 (1977).
- [14] G. Deco, V. K. Jirsa, P. A. Robinson, M. Breakspear, K. Friston, and O. Sporns, The dynamic brain: From spiking neurons to neural masses and cortical fields, *PLoS Comput. Biol.* **4**, e1000092 (2008).
- [15] S. Coombes, Large-scale neural dynamics: Simple and complex, *NeuroImage* **52**, 731 (2010).
- [16] *Principles of Neural Science*, 5th ed., edited by J. Hudspeth, T. M. Jessell, E. R. Kandel, and J. H. Schwartz (McGraw-Hill, New York, 2013).
- [17] O. Sporns and G. Tononi, Classes of network connectivity and dynamics, *Complexity* **7**, 28 (2002).
- [18] *Handbook of Brain Connectivity*, edited by V. K. Jirsa and A. R. McIntosh (Springer-Verlag, Berlin, 2007).
- [19] *Micro-, Meso- and Macro-Connectomics of the Brain*, edited by H. Kennedy, D. C. Van Essen, and Y. Christen, Research and Perspectives in Neurosciences (Springer, Berlin, 2016).
- [20] E. T. Bullmore, A. Fornito, and A. Zalesky, *Fundamentals of Brain Network Analysis* (Academic Press, London, 2016).
- [21] M. Rubinov and O. Sporns, Complex network measures of brain connectivity: Uses and interpretations, *NeuroImage* **52**, 1059 (2010).
- [22] P. E. Roland, C. C. Hilgetag, and G. Deco, Tracing evolution of spatio-temporal dynamics of the cerebral cortex: Cortico-cortical communication dynamics, *Front. Syst. Neurosci.* **8**, 76 (2014).
- [23] I. Bojak and D. T. J. Liley, Axonal velocity distributions in neural field equations, *PLoS Comput. Biol.* **6**, e1000653 (2010).
- [24] F. M. Atay and A. Hutt, Neural fields with distributed transmission speeds and long-range feedback delays, *SIAM J. Appl. Dyn. Sys.* **5**, 670 (2006).
- [25] F. M. Atay and A. Hutt, Stability and bifurcations in neural fields with finite propagation speed and general connectivity, *SIAM J. Appl. Math.* **65**, 644 (2005).
- [26] P. L. Nunez and R. Srinivasan, Neocortical dynamics due to axon propagation delays in cortico-cortical fibers: EEG traveling and standing waves with implications for top-down influences on local networks and white matter disease, *Brain Res.* **1542**, 138 (2014).
- [27] V. K. Jirsa and M. Ding, Will a Large Complex System with Time Delays Be Stable? *Phys. Rev. Lett.* **93**, 070602 (2004).
- [28] V. K. Jirsa, Connectivity and dynamics of neural information processing, *Neuroinformatics* **2**, 183 (2004).
- [29] P. C. Bressloff, Spatiotemporal dynamics of continuum neural fields, *J. Phys. A: Math. Theor.* **45**, 033001 (2012).
- [30] D. Pinotsis, P. Robinson, P. beim Graben, and K. Friston, Neural masses and fields: Modeling the dynamics of brain activity, *Front. Comput. Neurosci.* **8**, 149 (2014).
- [31] *Neural Fields: Theory and Applications*, edited by S. Coombes, P. beim Graben, J. Potthast, and J. Wright (Springer, London, 2014).
- [32] P. L. Nunez and R. Srinivasan, *Electric Fields of the Brain* (Oxford University Press, New York, 2006).
- [33] G. Buzsaki, *Rhythms of the Brain* (Oxford University Press, New York, 2006).
- [34] S. Coombes, Waves and bumps and patterns in neural field theories, *Biol. Cybernetics* **93**, 91 (2005).
- [35] P. C. Bressloff, *Waves in Neural Media: From Single Neurons to Neural Fields* (Springer, London, 2014).
- [36] V. K. Jirsa, Neural field dynamics with local and global connectivity and time delay, *Philos. Trans. R. Soc. A* **367**, 1131 (2009).
- [37] V. K. Jirsa and J. A. S. Kelso, Spatiotemporal pattern formation in neural systems with heterogeneous connection topologies, *Phys. Rev. E* **62**, 8462 (2000).
- [38] M. R. Qubbaj and V. K. Jirsa, Neural Field Dynamics with Heterogeneous Connection Topology, *Phys. Rev. Lett.* **98**, 238102 (2007).
- [39] P. A. Robinson, P. N. Loxley, S. C. O'Connor, and C. J. Rennie, Modal Analysis of Corticothalamic Dynamics, Electroencephalographic Spectra, and Evoked Potentials, *Phys. Rev. Lett.* **63**, 041909 (2001).
- [40] B. Fisch, M. I. Sereno, and A. M. Dale, Cortical surface-based analysis II: Inflation, flattening, and a surface-based coordinate system, *NeuroImage* **9**, 195 (1999).
- [41] M. J. Kwon, J. Hahn, and H. W. Park, A fast spherical inflation method of the cerebral cortex by deformation of a simplex mesh on the polar coordinates, *Int. J. Imaging Syst. Technol.* **18**, 9 (2008).
- [42] S. C. O'Connor and P. A. Robinson, Spatially uniform and nonuniform analyses of electroencephalographic dynamics, with application to the topography of the alpha rhythm, *Phys. Rev. E* **70**, 011911 (2004).
- [43] B. M. Wingeier, P. L. Nunez, and R. B. Silberstein, Spherical harmonic decomposition applied to spatial-temporal analysis of human high-density electroencephalogram, *Phys. Rev. E* **64**, 051916 (2001).
- [44] P. A. Robinson, J. C. Pages, N. C. Gabay, T. Babaie, and K. N. Mukta, Neural field theory of perceptual echo and implications for estimating brain connectivity, *Phys. Rev. E* **97**, 042418 (2018).
- [45] S. Visser, R. Nicks, O. Faugeras, and S. Coombes, Standing and travelling waves in a spherical brain model: The Nunez model revisited, *Physica D* **349**, 27 (2017).
- [46] S. S. Sivakumar, A. G. Namath, and R. F. Galan, Spherical harmonics reveal standing EEG waves and long-range neural synchronization during non-REM sleep, *Front. Comput. Neurosci.* **10**, 59 (2016).
- [47] V. K. Jirsa and H. Haken, A derivation of a macroscopic field theory of the brain from the quasi-microscopic neural dynamics, *Phys. D: Nonlin. Phen.* **99**, 503 (1997).
- [48] S. Coombes, N. A. Venkov, L. Shiao, I. Bojak, D. T. J. Liley, and C. R. Laing, Modeling electrocortical activity through improved local approximations of integral neural field equations, *Phys. Rev. E* **76**, 051901 (2007).
- [49] M. E. Rose, *Elementary Theory of Angular Momentum* (Chapman & Hall, London, 1957).
- [50] Connectivity matrices are available, for instance, at <http://www.thevirtualbrain.org>
- [51] S. Petkoski and V. K. Jirsa, Transmission time delays organize the brain network synchronization, *Philos. Trans. R. Soc. A* **377**, 20180132 (2019).
- [52] S. Petkoski, A. Spiegler, T. Proix, P. Aram, J. J. Temprado, and V. K. Jirsa, Heterogeneity of time delays determines

- synchronization of coupled oscillators, [Phys. Rev. E \*\*94\*\*, 012209 \(2016\)](#).
- [53] T. B. Janvier and P. A. Robinson, Neural field theory of corticothalamic prediction with control systems analysis, *Front. Hum. Neurosci.* **10**, 3389 (2018).
- [54] D. Yang and P. A. Robinson, Critical dynamics of Hopf bifurcations in the corticothalamic system: Transitions from normal arousal states to epileptic seizures, [Phys. Rev. E \*\*95\*\*, 042410 \(2017\)](#).
- [55] F. Droste and B. Lindner, Exact analytical results for integrate-and-fire neurons driven by excitatory shot noise, [J. Comput. Neurosci. \*\*43\*\*, 81 \(2017\).](#)
- [56] P. A. Robinson, Neural field theory of synaptic plasticity, [J. Theor. Biol. \*\*285\*\*, 156 \(2011\).](#)